11-1-2020

Depletion of CLK2 sensitizes glioma stem-like cells to PI3K/mTOR and FGFR inhibitors.

Soon Young Park

Sandeep Mittal

Jianwen Dong

Kangjin Jeong

Emmanuel Martinez-Ledesma

See next page for additional authors

Authors

Soon Young Park, Sandeep Mittal, Jianwen Dong, Kangjin Jeong, Emmanuel Martinez-Ledesma, Yuji Piao, Sabbir Khan, Verlene Henry, Roel G W Verhaak, Nazanin Majd, Veerakumar Balasubramaniyan, and John F de Groot

Am J Cancer Res 2020;10(11):3765-3783
www.ajcr.us /ISSN:2156-6976/ajcr0111121

Original Article

Depletion of CLK2 sensitizes glioma stem-like cells to PI3K/mTOR and FGFR inhibitors

Soon Young Park[1], Sandeep Mittal[2], Jianwen Dong[2], Kangjin Jeong[1], Emmanuel Martinez-Ledesma[2], Yuji Piao[2], Sabbir Khan[2], Verlene Henry[3], Roel GW Verhaak[4], Nazanin Majd[2], Veerakumar Balasubramaniyan[2], John F de Groot[2]

[1]Department of Cell Developmental and Cancer Biology, Oregon Health and Science University, Portland, Oregon, USA; [2]Department of Neuro-Oncology, The University of Texas MD Anderson Cancer Center, Houston, Texas, USA; [3]Department of Neuro-Surgery, The University of Texas MD Anderson Cancer Center, Houston, Texas, USA; [4]The Jackson Laboratory for Genomic Medicine, Farmington, Connecticut, USA

Received March 19, 2020; Accepted September 10, 2020; Epub November 1, 2020; Published November 15, 2020

Abstract: The Cdc2-like kinases (CLKs) regulate RNA splicing and have been shown to suppress cell growth. Knockdown of CLK2 was found to block glioma stem-like cell (GSC) growth *in vivo* through the AKT/FOXO3a/p27 pathway without activating mTOR and MAPK signaling, suggesting that these pathways mediate resistance to CLK2 inhibition. We identified CLK2 binding partners using immunoprecipitation assays and confirmed their interactions *in vitro* in GSCs. We then tested the cellular viability of several signaling inhibitors in parental and CLK2 knockdown GSCs. Our results demonstrate that CLK2 binds to 14-3-3τ isoform and prevents its ubiquitination in GSCs. Stable CLK2 knockdown increased PP2A activity and activated PI3K signaling. Treatment with a PI3K/mTOR inhibitor in CLK2 knockdown cells led to a modest reduction in cell viability compared to drug treatment alone at a lower dose. However, FGFR inhibitor in CLK2 knockdown cells led to a decrease in cell viability and increased apoptosis. Reduced expression of CLK2 in glioblastoma, in combination with FGFR inhibitors, led to synergistic apoptosis induction and cell cycle arrest compared to blockade or either kinase alone.

Keywords: CLK2, FGFR, PI3K/mTOR, glioblastoma, glioma stem cells, survival

Introduction

Receptor tyrosine kinases are cell surface receptors that orchestrate major signaling pathways such as Ras/MAPK/ERK and Ras/PI3K/AKT [1]. The receptor tyrosine kinase family includes six tyrosine kinase receptors; of these, epidermal growth factor (EGFR) and the structurally related ErbB2/HER2 are amplified and mutated in 45%-57% and 8%-41% of glioblastoma patients, respectively [2, 3]. Another receptor of the tyrosine kinase family, fibroblast growth factor receptor (FGFR), is amplified in a subset of 3.2% of glioblastoma cases, as reported by The Cancer Genome Atlas studies [3]. These receptor tyrosine kinases downstream signaling pathways are involved in the regulation of various cellular processes, including cell proliferation, survival, and differentiation.

Upon the activation of EGFR and FGFR, activated AKT phosphorylates, both the FOXO family, which inhibits pro-apoptotic signaling, and the mammalian target of rapamycin (mTOR)/S6-kinase pathways; this results in increased cell proliferation and tumor growth. Cancer cells maintain mTOR activation despite suppressed PI3K/AKT signaling [4]. Therefore, dual PI3K/mTOR inhibitors have improved therapeutic effects on tumor cells compared with either inhibitor alone and are currently being tested in clinical trials. GSK2126458 is a dual PI3K/mTOR inhibitor that was evaluated in a phase 1 clinical trial in solid tumors and lymphoma in 2017 [5]. Activation of Ras changes GDP to GTP and regulates MAP kinase and ERK phosphorylation. Inhibitors and antibodies targeting these pathways have had varied success in the treatment of glioblastoma [6]. Despite preclinical and early-phase clinical testing of various spe-

cific tyrosine kinase pathway inhibitors, targeting these pathways in glioblastoma had limited success in the clinic. More effective therapies targeting critical signaling elements in glioblastoma are needed to prolong the survival of patients with this deadly disease.

In our previous study, we found that CLK2 was expressed at high levels in glioblastoma, where it regulates the AKT/FOXO3a/p27 pathway [7]. High expression of CLK2 in glioblastoma tissue is correlated with poor outcome. Although CLK2 depletion was found to be beneficial for survival in preclinical glioblastoma models, several other signaling cascades remain activated. In cases of insulin-induced AKT activation, CLK2 phosphorylates the phosphatase 2A (PP2A) regulatory subunit B56β, which dephosphorylates the phosphor AKT site (S473 and T308) [8]. Heterodimeric PP2A is formed from the combination of three subunits: a catalytic subunit (C), a regulatory subunit (B), and scaffolding (A) [9]. Among the B subunits, B55 is important in PP2A's specificity for AKT [10]. Proteasome inhibition results in an accumulation of CLK2 in neurons, but not in Shank3-deficient neurons [11, 12]. In addition, CLK2 inhibition has been shown to result in reduced tumor growth and proliferation in MYC-amplified breast cancer [13]. Given the central role of CLKs in the phosphorylation of serine/arginine-rich proteins, which control a wide variety of cellular functions such as splicing and protein stabilization, it is vital to study specific CLK functions in cancer cells.

14-3-3 protein has known modulatory functions that regulate multiple signaling pathways through binding with Ser/Thr-phosphorylated motifs on the target protein [14]. The protein has several isoforms, with at least seven (β, γ, ε, σ, ζ, τ, and η) in mammals [15]. Depending on the binding target protein, 14-3-3 protein affects the stability, localization, or association of target proteins [16]. The recognition motif between AKT and 14-3-3 overlap [17]. Several AKT target proteins are regulated by 14-3-3 protein, including FOXO protein, BAD p27Kip1, and YAP. Binding of 14-3-3 protein with FOXO is regulated via FOXO phosphorylation by AKT [18].

Given the various biological functions of CLK2 and its high expression level in solid tumors, including glioblastoma, a better mechanistic understanding of its regulation in cancer is vital for the development of CLK2-based targeted therapy. We hypothesized that CLK2 combination therapy with multiple molecularly targeted agents would be a promising approach to overcoming therapy resistance.

Materials and methods

Cell lines and reagents

We isolated glioma stem-like cells (GSCs) from brain tumor specimens and cultured them at The University of Texas MD Anderson Cancer Center (Houston, TX). Acquisition of these cells was approved by the Institutional Review Board of MD Anderson. Glioma stem cell development is funded by the MD Anderson Brain Cancer SPORE supported by P50CA127001. The GSCs were cultured in Dulbecco's modified Eagle's medium-F12 medium (1:1) with B27 (Invitrogen), basic fibroblast growth factor (bFGF; Sigma), and epidermal growth factor (EGF; Sigma) at 37°C in a humidified atmosphere of 5% CO_2 and 95% air. They were then tested and authenticated by DNA fingerprinting in the MD Anderson Cancer Center Cell Line Characterization Core. 293T embryonic kidney cells were obtained from the American Type Culture Collection (ATCC) and maintained in Dulbecco's modified Eagle medium (Sigma), supplemented with 10% fetal bovine serum. All cell lines were free of mycoplasma contamination. Inhibitors of PI3K/mTOR1/2 (omipalisib [GSK2126458]; cat. #S2658), PI3K (BKM120; cat. #S2247), FGFR (LY2874455; cat. #S7057), and MEK (PD98059; cat. #S1177) were purchased from Selleckchem. Okadaic acid (cat. #495604) was purchased from Calbiochem.

Stable knockdown and overexpression of CLK2 or knockdown of 14-3-3τ in GSCs

CLK2 inhibition in GSCs by shRNA mediated approaches have been described previously [7]. CLK2 lentiviral activation particles were purchased from Santa Cruz (sc-403326-LAC). 14-3-3τ was purchased from Sigma (TRCN-0000078172).

Cell viability

For the cell viability assay, 5×10^3 GSCs per well were cultured with specific inhibitors for 5 days in a 96-well plate. A cell viability analysis was performed using a CellTiter-Glo lumines-

cent cell viability assay (Promega), according to the manufacturer's protocol.

Cell cycle analysis and apoptosis assay

Vector-infected and CLK2 knockdown GSCs with specific inhibitors were incubated for 1 day (cell cycle) or 3 days (apoptosis). For the cell cycle analysis, cells were treated with a natural enzyme mixture (Accutase; Sigma), washed with 1 × phosphate-buffered saline (PBS), fixed, and permeabilized with cold 70% EtOH for 24 hours at -20°C. After incubation, cells were washed three times with 1 × PBS and incubated with 500 µl of propidium iodide (BD Biosciences) for 30 minutes at 37°C. A flow cytometric analysis was performed using at least 10,000 cells, and the cell cycle phases were analyzed using a FACSCalibur flow cytometer (BD Biosciences). For the apoptosis assay, we used $5*10^5$/100 µl of resuspended cells in Annexin V binding buffer, stained with 2 µl of Annexin V-APC (Biolegend) and 1 µg/ml of DAPI for 15 minutes at ambient temperature. Apoptosis was analyzed at the MD Anderson Flow Cytometry and Cellular Imaging Facility.

PP2A immunoprecipitation phosphatase assay

PP2A activity (cat. #17-313) was determined using the PP2A immunoprecipitation phosphatase assay kit from Millipore. The lysed cells were rotated for 2 h at 4°C with 4 µg of anti-PP2A and protein agarose. After being washed three times, the cells were incubated for 10 min in a 30°C shaking incubator with 60 µl of phosphopeptide and 20 µl of Ser/Thr assay buffer. The supernatant of the reaction (25 µl) was incubated with 100 µl of malachite green phosphate detection solution for 15 minutes and read at 650 nm.

Animal xenografts

In the *in vivo* experiments, we used 8 to 10-week-old female nude mice that had been strictly inbred at MD Anderson and maintained in the MD Anderson Research Animal Support Facility in accordance with Institute of Laboratory Animal Research standards. The GSC7-2 and GSC272 cells (5×10^5) were implanted intracranially into the mice, as described previously [19]. After 3 days, GSK212458 (1.5 mg/kg, dissolved in 1% DMSO/30% polyethylene glycol/1% Tween 80) or LY2874455 (3 mg/kg, dissolved in 2% DMSO/30% PEG-300/5% Tween 80) was administered intra-gastrically once daily for 5 days/week. All animal experiments were approved by the MD Anderson Institutional Animal Care and Use Committee. Mice that became moribund with neurological symptoms were euthanized. Tumor volumes were calculated using the formula [(width) × (width) × (length)]/2. A survival analysis was conducted using the Kaplan-Meier method. The mice's tumor volumes were analyzed using an unpaired two-tailed Student *t*-test, and their survival durations were compared using the log-rank test.

Western blot analysis

GSCs were lysed using RIPA lysis buffer (Cell Signaling Technology), and samples were subjected to sodium dodecyl sulfate-polyacrylamide gel electrophoresis. The separated proteins were electrophoretically transferred to polyvinylidene fluoride membranes. Blots were incubated with a primary antibody overnight at 4°C and then incubated with horseradish peroxidase-linked secondary anti-rabbit or anti-mouse antibodies (Bio-Rad). Antibodies against phosphorylated AKT (cat. #13038), AKT (cat. #9272), phosphorylated mTOR (cat. #2971), phosphorylated S6 (cat. #4858), phosphorylated 4EBP1 (cat. #9456), phosphorylated ERK (cat. #9101), ERK (cat. #9102), 14-3-3 Family Antibody Sampler Kit (cat. #9769), K48-linkage-specific polyubiquitin (cat. #8081), phosphorylated FOXO3a (cat. #9465), and FOXO3a (cat. #2497) were purchased from Cell Signaling Technology. CLK2 (cat. #HPA055366), 14-3-3τ (cat. #SAB2500002), and α-tubulin (cat. #T9026) were purchased from Sigma-Aldrich. Phosphorylated FGFR1 (cat. #PAB0472) and HIF-1alpha (cat. #610958) were purchased from Abnova and BD Biosciences. Antibodies of phosphor PP2A (cat. #1155-1) and PP2A (cat. #1512-1) were purchased from Epitomics. The results of three independent western blot experiments, performed in triplicate, are reported.

Immunohistochemical, immunofluorescence, and TUNEL assays

Single cells were plated on precoated poly-L-lysine coverslips, fixed in methanol for 15 minutes at -20°C, rinsed with PBS at least three times, blocked in 5% goat serum with 0.2%

Triton X-100 for 1 hour, and incubated with specific antibody overnight. The next day, the slides were washed at least three times with PBS and 0.2% Triton X-100 and incubated with secondary antibody for 1 hour. The slides were then washed three times and mounted. Patient brain tissue samples were fixed in 4% paraformaldehyde for 24 hours, embedded in paraffin, sectioned serially (4 μm), and stained with hematoxylin and eosin (Sigma-Aldrich).

For immunohistochemical staining, slides were deparaffinized and subjected to graded rehydration. After 3% serum blocking and antigen retrieval (citrate buffer, pH 6.0), the slides were incubated with primary antibodies overnight at 4°C. After the slides had been washed in PBS with Tween 20, the primary antibody reactions were detected using a VECTASTAIN ABC kit (Vector Laboratories) with the respective secondary antibodies. For immunofluorescence studies, after blocking, tissue sections were incubated with an antibody overnight at 4°C. Secondary antibodies (Invitrogen) were incubated for 1 hour at ambient temperature. Antibodies against HIF-1alpha (cat. 610958; BD Biosciences), CLK2 (cat. #ab188141; Abcam), and 14-3-3τ (cat. #9638, Cell Signaling Technology) were used in the immunohistochemical and immunofluorescence assays. The results of three independent experiments performed in triplicate are reported. For TUNEL assays in xenografts, slides were examined according to the manufacturer's protocol (in situ cell death detection kit, TMR red; Roche).

Detection of multiple signaling pathways using reverse-phase protein array

The cells were incubated with specific inhibitors for 3 days, and the protein was collected following reverse phase protein array (RPPA) sample preparation methods. Samples were probed with 279 validated primary antibodies for analysis at the MD Anderson Functional Proteomics RPPA.

Clonogenic formation assay

To evaluate clonogenic formation, we seeded GSCs at 5 cells per well in 96-well plates with low-dose inhibitors for 3-4 weeks, in triplicate. Wells with neurospheres (> 100 μM) were counted as positive, and wells without spheres as negative. The percentages of positive neurospheres in each plate were compared among different treatment groups.

Statistical analysis

All statistical analyses were conducted using the InStat software program for Microsoft Windows (GraphPad software). Data were reported as the mean ± standard deviation. All other data were compared using an unpaired two-tailed Student *t*-test.

Results

CLK2 regulated AKT phosphorylation through PP2A activity

CLK2 regulates AKT/FOX3a phosphorylation in GSCs [7]. The PP2A holoenzyme comprises a structural A subunit, a regulatory B subunit, and a catalytic C subunit [9]. Several kinds of B subunit exist: B55 is important to PP2A's specificity for AKT [10], and B56β mediates the insulin-regulated assembly of the PP2A phosphotase holoenzyme complex with CLK2 [8].

Treatment with an ATP-competitive CLK2 inhibitor (TG003) resulted in decreased phosphorylation of AKT T308 and FOXO3a at 40 μM in GSCs (**Figure 1A**). To understand the CLK2-mediated inhibition of AKT phosphorylation, we first determined its upstream regulator PP2A. PP2A signaling was determined using a PP2A immunoprecipitation phosphatase assay kit. As shown in **Figure 1B**, PP2A inhibitor (okadaic acid [OA]) significantly inhibited PP2A activity, whereas PI3K inhibitor (BKM120) had no effect. We confirmed these results in the cell lysate used for the phosphatase activity assay using a PP2A-specific antibody. PP2A inhibition increased AKT phosphorylation at T308. Furthermore, we investigated the role of PP2A in CLK2 by using CLK2 knockdown cells; depletion of CLK2 increased PP2A activity (**Figure 1B**). Consistent with these results, overexpression of CLK2 in GSC272 cells resulted in suppression of PP2A activity (**Figure 1C**) and increased cytosolic FOXO3a phosphorylation (**Figure 1D**). Overall, these results indicate that CLK2 regulates PP2A activity in brain tumor cancer stem cells.

14-3-3τ regulates the stabilization of CLK2

14-3-3 proteins are a family of conserved modulator proteins that regulate multiple signaling pathways, including AKT and FOXO3a. 14-3-3 proteins binds in specific Ser/Thr-phosphorylated motifs on target proteins [12]. Depending

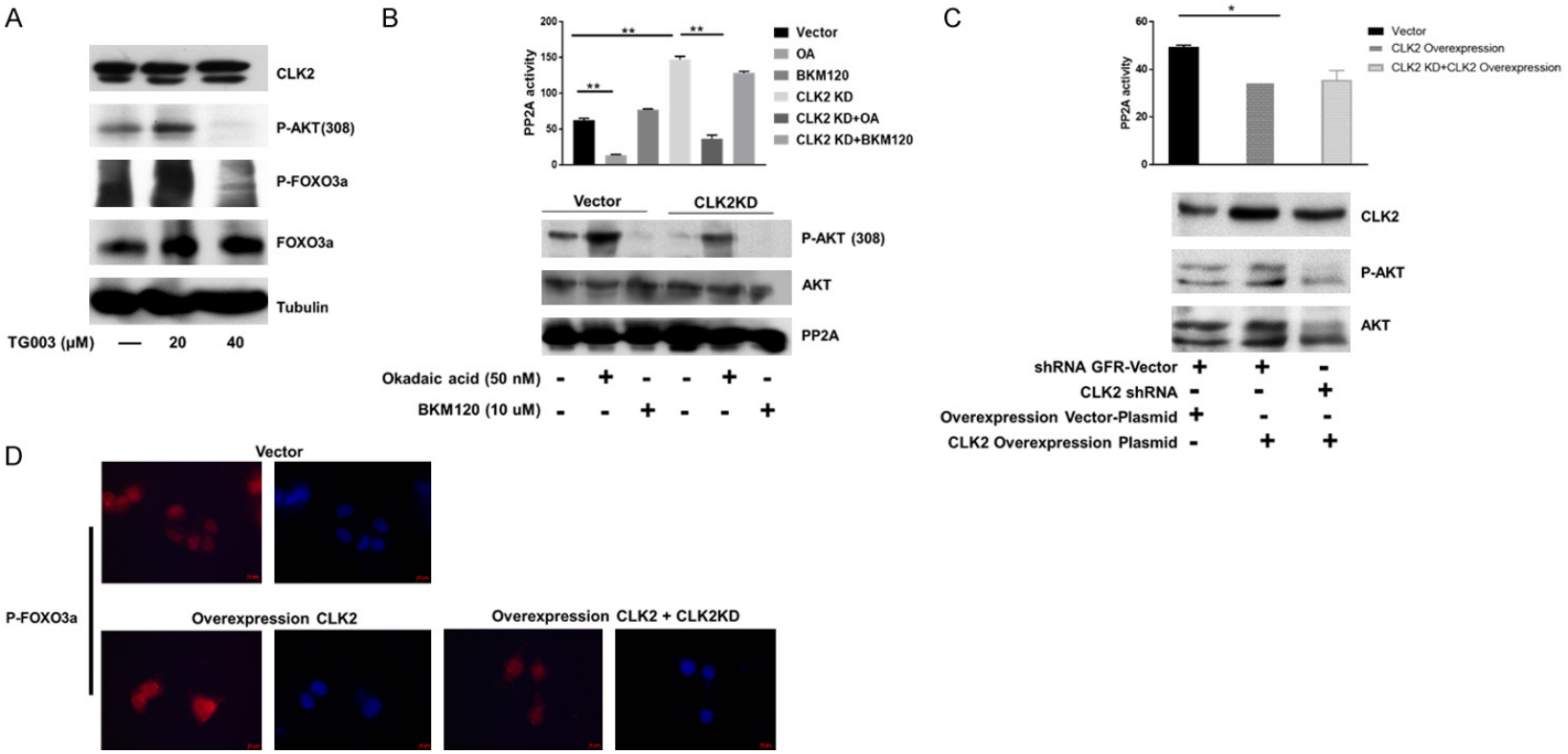

Figure 1. CLK2 regulated PP2A activity in GSCs. (A, B) GSC272 cells were treated with the indicated inhibitors-TG003 (CLK inhibitor), OA (PP2A inhibitor), and BKM120 (PI3K inhibitor)-for 24 hours and assessed by Western blot analysis and a PP2A activity assay. (C) PP2A activity and FOXO3a phosphorylation were assessed using a PP2A activity assay and (D) an immunofluorescence assay in GSC272 vector, CLK2-overexpressing, and CLK2 knockdown and CLK2-overexpressing cells. CLK2, PP2A, and phosphor AKT levels were detected by Western blot analysis. *P < 0.05, **P < 0.01.

on target binding, 14-3-3 modulates target protein activity, stability, cellular location, or association [16, 20]. We determined the binding affinity of CLK2 with the 14-3-3 isotype; CLK2 binds with 14-3-3τ, 14-3-3α/β, and PP2A in 293T cells (**Figure 2A**). Increasing CLK2 expression resulted in continued binding affinity with 14-3-3τ but decreased affinity with PP2A (**Figure 2B**). Overexpression of CLK2 resulted in greater binding affinity with 14-3-3τ but not with 14-3-3α/β (no change) compared with GSC272 vector and less binding affinity with phospho-PP2A (**Figure 2C**). In contrast, lower levels of CLK2 in CLK2 shRNA cells led to decreased binding affinity with 14-3-3τ and increased binding affinity with phospho-pp2A (**Figure 2D**). Furthermore, CLK2 co-localized with 14-3-3τ, as revealed by an immunofluorescence analysis (**Figure 2E**). Interestingly, there was no direct binding of 14-3-3τ with PP2A in the presence of CLK2 in GSCs (Data not shown). Since ubiquitination and proteasomal degradation regulate CLK2 protein stability [11, 21], we determined CLK2 stability in the absence of 14-3-3τ. Depletion of 14-3-3τ resulted in high levels of ubiquitination on CLK2 compared with that in control cells (**Figure 2F**), whereas proteasome inhibition stimulated the expression of CLK2 in control cells but not in 14-3-3τ cells (**Figure 2G**). Overall, our results suggest that CLK2 stabilization is regulated by 14-3-3τ in glioma stem cells.

PI3K/mTOR and FGFR inhibitors demonstrate synergistic effects on CLK2 knockdown glioma stem cell viability

In the present study, we identified therapies that are synergistic against glioblastoma when combined with CLK2 knockdown. Inhibitors of mTOR, FGFR, EGFR, and ERK were tested in parental and CLK2 knockdown glioma stem-like cell lines (**Figure 3A**). In GSC7-2, GSC272, and GSC20 cells, treatment with mTOR inhibitor (GSK2126458) in CLK2 knockdown cell lines led to significant reductions in cell viability compared to drug treatment alone at a lower dose. Furthermore, the combination of FGFR inhibitor (LY2874455) and CLK2 knockdown decreased viability synergistically in GSC7-2 and GSC272 cells, at a high concentration. EGFR and MEK inhibitors had no combined effect in the viability assay. Depletion of CLK2 induced G1 phase cell cycle arrest, and the combination of CLK2 knockdown and mTOR inhibitor or FGFR inhibitors increased sub-G1 phase, suggesting apoptosis induction (**Figure 3B**).

To determine whether PI3K/mTOR and FGFR inhibitors induce apoptosis in CLK2 knockdown cell lines, we performed an annexin V/DAPI assay in control and CLK2 knockdown GSCs, with and without inhibitor (**Figure 3C**). PI3K/mTOR and FGFR inhibitors induced apoptosis in a dose-dependent manner. Treatment with FGFR inhibitors in CLK2 knockdown cell lines led to synergistic apoptosis induction compared to drug treatment alone. Treatment with inhibitors in CLK2 knockdown lines led to decreased colony formation compared to drug treatment alone in GSC7-2 cells (**Figure 3D**). Our findings suggest that the combination of CLK2 knockdown and PI3K/mTOR or FGFR inhibitors synergistically induces apoptosis in GSCs.

Effect of PI3K/mTOR (GSK2126458) and FGFR (LY2874455) inhibitors on GSC viability

We first examined the inhibitory effect of GSK2126458 and LY2874455 in glioma stem cells. GSK2126458, a dual PI3K/mTOR, had the lowest IC_{50} values for all the GSCs tested (< 0.5 μM) (**Figure 4A**). The response of LY2874455, an FGFR inhibitor, to FGFR inhibition was found to be cell line specific (**Figure 4A**). GSC262, GSC280, GSC11, GSC23, GSC-274, GSC7-2, GSC231, GSC295, and GSC300 cells were the most responsive, with IC_{50s} of < 3 μM; GSC272, GSC8-11, GSC6-27, GSC20, GSC17, and GSC28 cells were the most resistant, with IC_{50s} of > 3 μM.

To confirm that the drug targets are expressed and modulated by drug treatment, we evaluated PTEN and FGFR by real-time PCR (**Figure 4B**). PTEN expression levels were correlated with the IC_{50s} of GSK2126458. The more sensitive cell lines had higher total expression levels of FGFR1 than did the resistant cell lines.

We determined relative protein expression levels after treatment with the IC_{50} dose of inhibitor using RPPA (**Figure 4C**). Phosphorylation of mTOR, AKT, S6 kinase (ribosomal protein S6), and 4EBP1 (eukaryotic initiation factor 4E binding protein 1) was decreased in a dose-dependent manner following treatment with

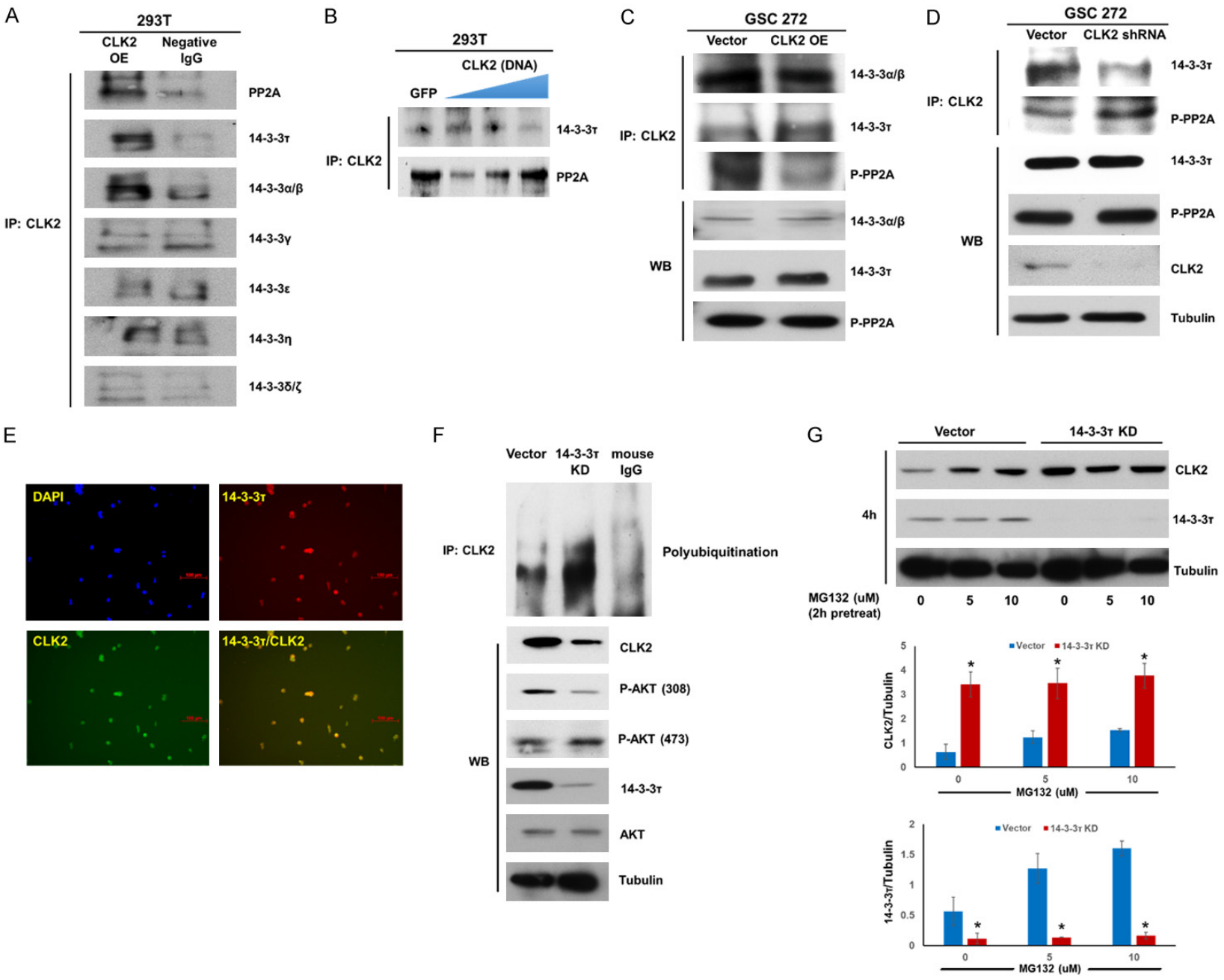
A
293T
CLK2 OE
Negative IgG
IP: CLK2
PP2A
14-3-3τ
14-3-3α/β
14-3-3γ
14-3-3ε
14-3-3η
14-3-3δ/ζ
B
293T
CLK2 (DNA)
GFP
IP: CLK2
14-3-3τ
PP2A
C
GSC 272
Vector
CLK2 OE
IP: CLK2
14-3-3α/β
14-3-3τ
P-PP2A
WB
14-3-3α/β
14-3-3τ
P-PP2A
D
GSC 272
Vector
CLK2 shRNA
IP: CLK2
14-3-3τ
P-PP2A
WB
14-3-3τ
P-PP2A
CLK2
Tubulin
E
DAPI
14-3-3τ
CLK2
14-3-3τ/CLK2
F
Vector
14-3-3τ KD
mouse IgG
IP: CLK2
Polyubiquitination
WB
CLK2
P-AKT (308)
P-AKT (473)
14-3-3τ
AKT
Tubulin
G
Vector
14-3-3τ KD
4h
CLK2
14-3-3τ
Tubulin
MG132 (uM)
(2h pretreat)
0
5
10
0
5
10
Vector
14-3-3τ KD
CLK2/Tubulin
MG132 (uM)
14-3-3τ/Tubulin
MG132 (uM)

Figure 2. CLK2 binding with 14-3-3τ increased stability via a degradation mechanism. A-F. CLK2-overexpressing 293T cells, CLK2-overexpressing or CLK2 knockdown GSC272 cells, and 14-3-3τ knockdown GSC272 cells were collected and assessed using an immunoprecipitation assay and immunofluorescence staining. Representative images showed that showed that 14-3-3τ (red) co-localized with CLK2 (green) in GSC272 cells. The nucleus stained with DAPI, blue. G. GSC272 cells were pretreated with the indicated amounts of MG132 for 2 hours in serum-free media, and bFGF/EGF was added at the same concentrations as complementary media for 4 hours. The bar graph shows densitometric quantification of western blot bands (n=2). *P < 0.05 compared to vector cells.

A

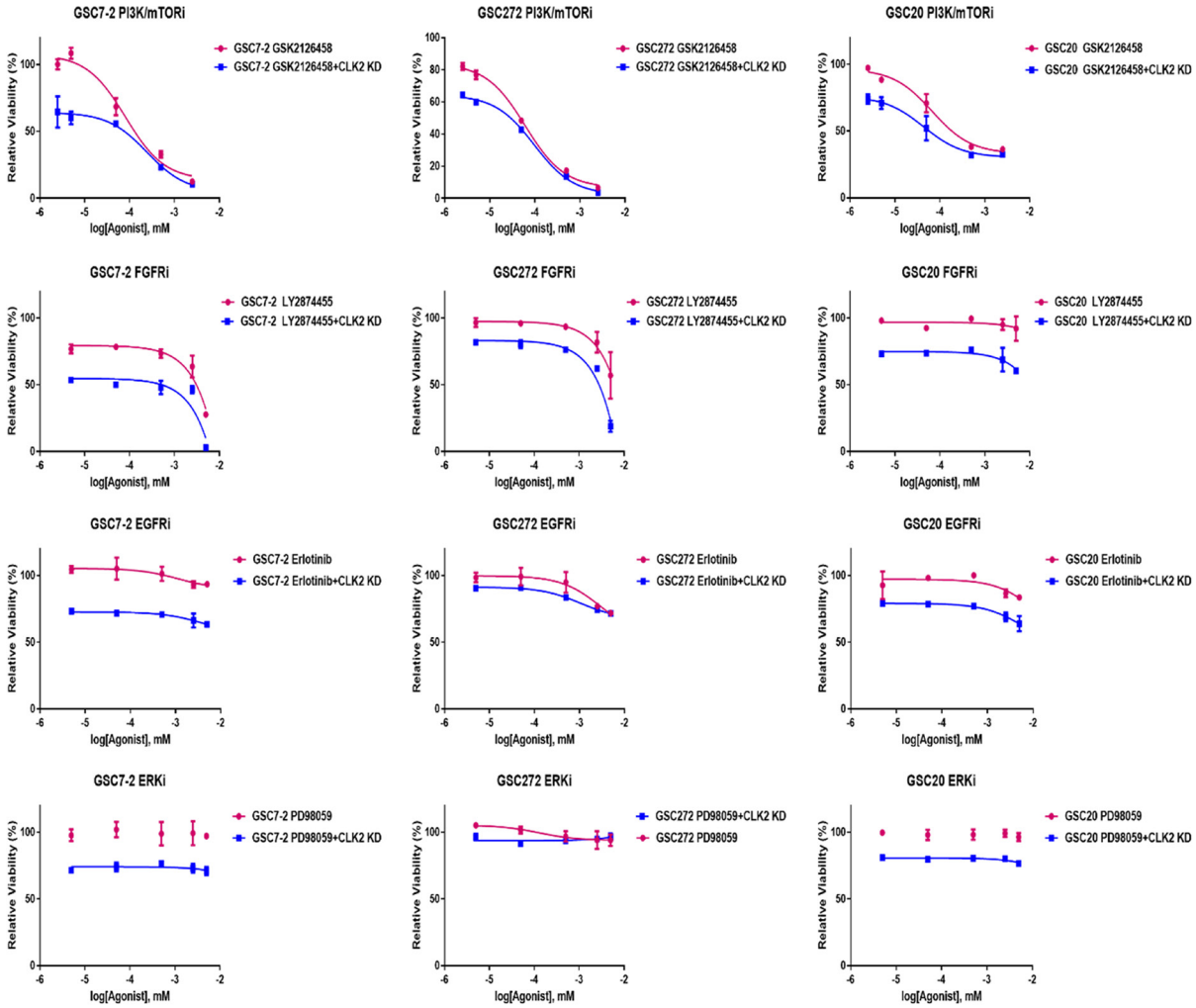

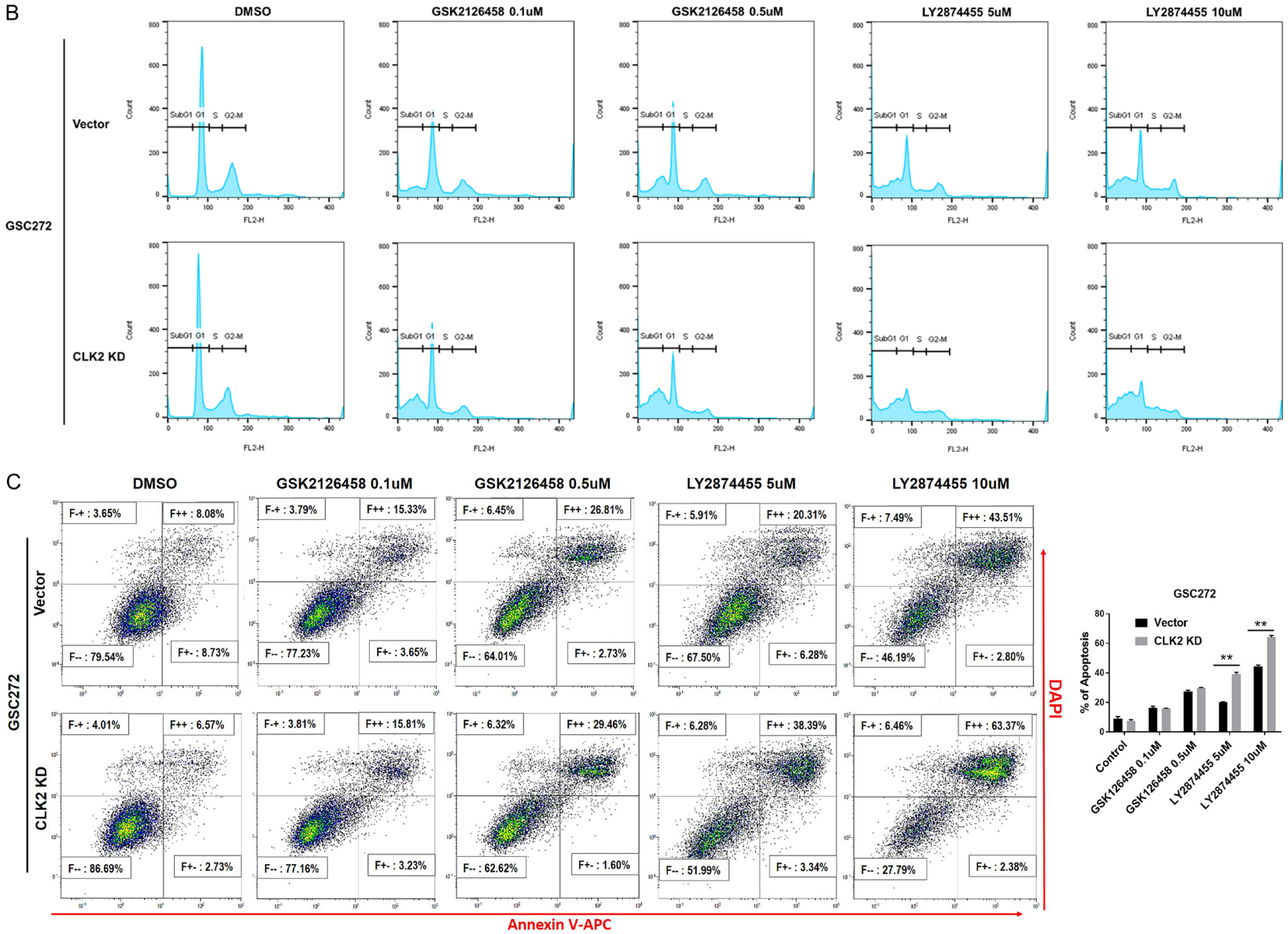
B
DMSO
GSK2126458 0.1uM
GSK2126458 0.5uM
LY2874455 5uM
LY2874455 10uM
GSC272
Vector
CLK2 KD
SubG1 G1 S G2-M
Count
FL2-H
C
DMSO
GSK2126458 0.1uM
GSK2126458 0.5uM
LY2874455 5uM
LY2874455 10uM
GSC272
Vector
CLK2 KD
F-+ : 3.65%
F++ : 8.08%
F-- : 79.54%
F+- : 8.73%
F-+ : 3.79%
F++ : 15.33%
F-- : 77.23%
F+- : 3.65%
F-+ : 6.45%
F++ : 26.81%
F-- : 64.01%
F+- : 2.73%
F-+ : 5.91%
F++ : 20.31%
F-- : 67.50%
F+- : 6.28%
F-+ : 7.49%
F++ : 43.51%
F-- : 46.19%
F+- : 2.80%
F-+ : 4.01%
F++ : 6.57%
F-- : 86.69%
F+- : 2.73%
F-+ : 3.81%
F++ : 15.81%
F-- : 77.16%
F+- : 3.23%
F-+ : 6.32%
F++ : 29.46%
F-- : 62.62%
F+- : 1.60%
F-+ : 6.28%
F++ : 38.39%
F-- : 51.99%
F+- : 3.34%
F-+ : 6.46%
F++ : 63.37%
F-- : 27.79%
F+- : 2.38%
DAPI
Annexin V-APC
GSC272
Vector
CLK2 KD
% of Apoptosis
**
**
Control
GSK126458 0.1uM
GSK126458 0.5uM
LY2874455 5uM
LY2874455 10uM

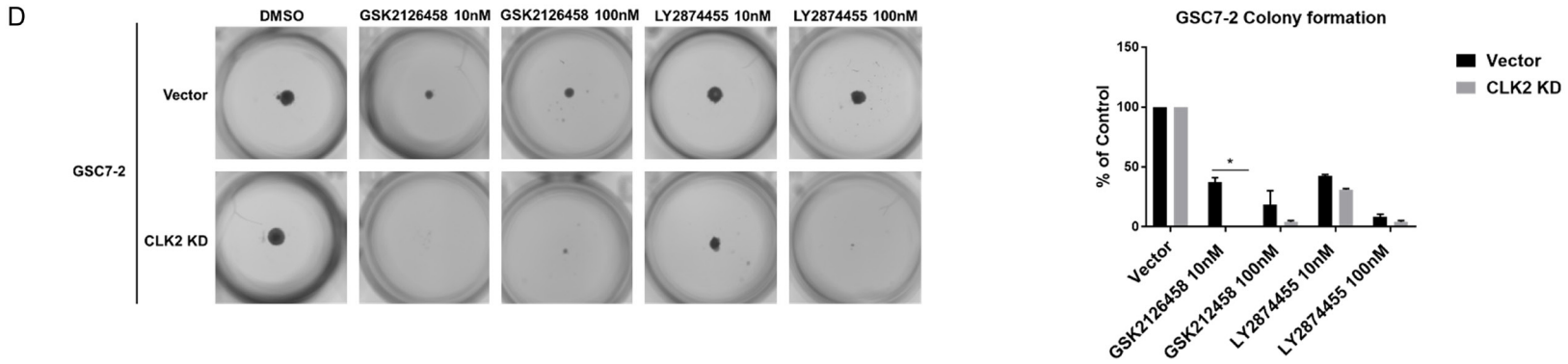

Figure 3. PI3K/mTOR or FGFR inhibitors decreased cell viability and the cell cycle in CLK2-depleted cells. A. GSCs were treated with inhibitors of EGFR (Tarceva), ERK (PD98059), PI3K/mTOR (GSK2124658), and FGFR (LY2874455) in vector and CLK2-depleted cells for 5 days (viability). Cell viability was detected by CellTiter-Glo. B, C. GSC272 cells were incubated with PI3K/mTOR (GSK2124658) and FGFR (LY2874455) for 1 day (cell cycle) or 3 days (apoptosis), collected, and washed two times. B. For cell cycle analysis, cells were incubated with 70% EtOH at -20°C for 1 day and washed three times with PBS and stained with propidium iodide. C. For apoptosis assay, the cells were stained with annexin V-APC, DAPI. Apoptosis and the cell cycle were detected using a FACS analysis. D. A colony formation assay was done in GSC 7-2 cells treated with lower dose of PI3K/mTOR and FGFR inhibitors. The results are presented as the percentage of the control. *P < 0.05, **P < 0.01.

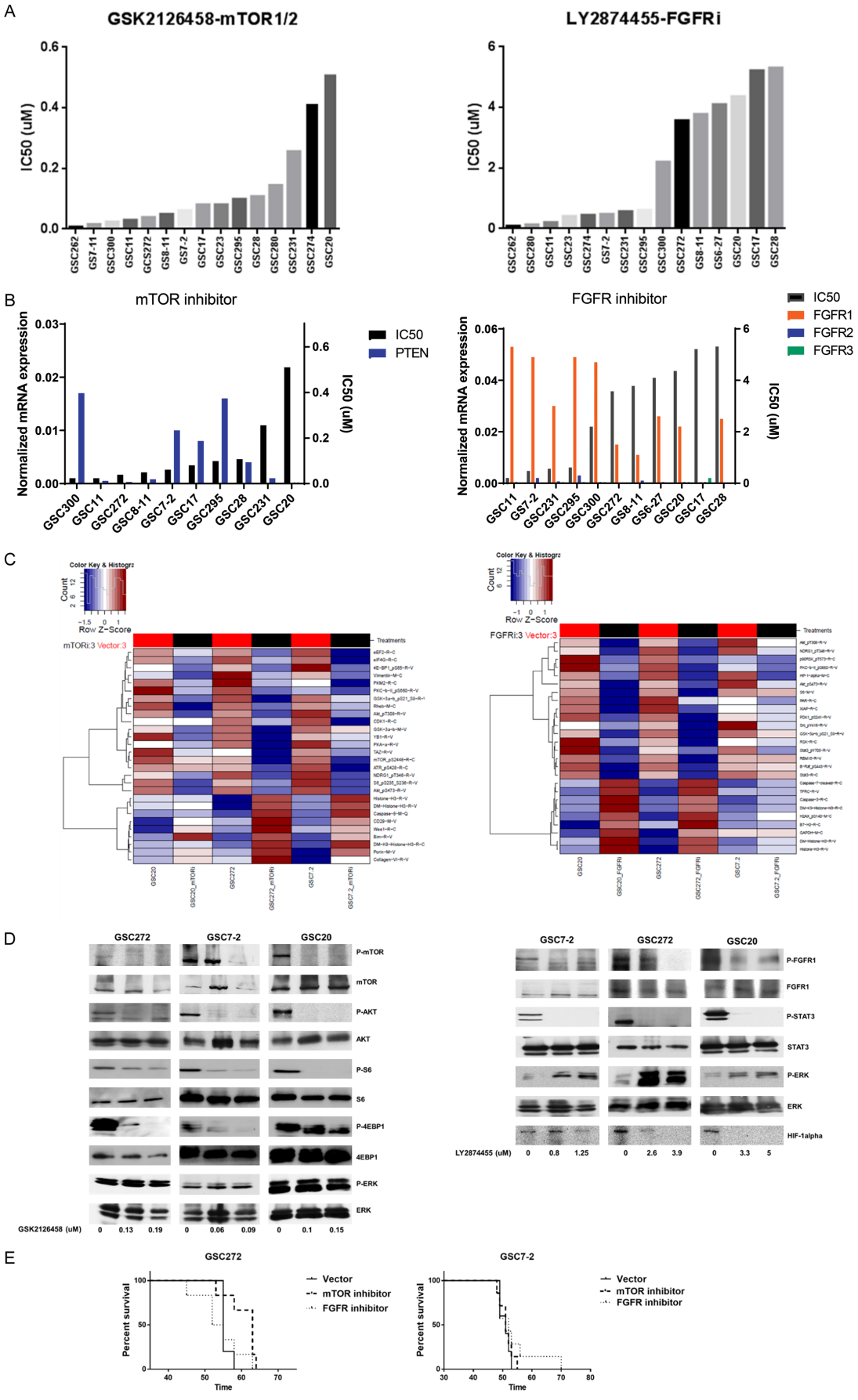
A
GSK2126458-mTOR1/2
IC50 (uM)
GSC262 GS7-11 GSC300 GSC11 GCS272 GS8-11 GS7-2 GSC17 GSC23 GSC295 GSC28 GSC280 GSC231 GSC274 GSC20
LY2874455-FGFRi
IC50 (uM)
GSC262 GSC280 GSC11 GSC23 GSC274 GS7-2 GSC231 GSC295 GSC300 GSC272 GS8-11 GS6-27 GSC20 GSC17 GSC28
B
mTOR inhibitor
Normalized mRNA expression
IC50 (uM)
IC50
PTEN
GSC300 GSC11 GSC272 GSC8-11 GSC7-2 GSC17 GSC295 GSC28 GSC231 GSC20
FGFR inhibitor
Normalized mRNA expression
IC50 (uM)
IC50
FGFR1
FGFR2
FGFR3
GSC11 GS7-2 GSC231 GSC295 GSC300 GSC272 GS8-11 GS6-27 GSC20 GSC17 GSC28
C
Color Key & Histogram
Count
Row Z-Score
mTORi:3 Vector:3
Treatments
GSC20 GSC20_mTORi GSC272 GSC272_mTORi GSC7-2 GSC7-2_mTORi
Color Key & Histogram
Count
Row Z-Score
FGFRi:3 Vector:3
Treatments
GSC20 GSC20_FGFRi GSC272 GSC272_FGFRi GSC7-2 GSC7-2_FGFRi
D
GSC272 GSC7-2 GSC20
P-mTOR
mTOR
P-AKT
AKT
P-S6
S6
P-4EBP1
4EBP1
P-ERK
ERK
GSK2126458 (uM) 0 0.13 0.19 0 0.06 0.09 0 0.1 0.15
GSC7-2 GSC272 GSC20
P-FGFR1
FGFR1
P-STAT3
STAT3
P-ERK
ERK
HIF-1alpha
LY2874455 (uM) 0 0.8 1.25 0 2.6 3.9 0 3.3 5
E
GSC272
Percent survival
Time
Vector
mTOR inhibitor
FGFR inhibitor
GSC7-2
Percent survival
Time
Vector
mTOR inhibitor
FGFR inhibitor

Figure 4. Effect of PI3K/mTOR or FGFR inhibitors on GSCs. A. Several GSCs were treated with serial doses of inhibitors for 5 days; a volume of CellTiter-Glo reagent was added, and the luminescence was recorded. B. The cells were collected, and PTEN and FGFR mRNA levels were determined by real-time PCR. C. The cells were treated with the IC_{50} value of inhibitors for 3 days, and the protein expression levels were analyzed by RPPA. Heatmaps from different proteins were used to compare treatment with no treatment and show the predicted targets of inhibitors. D. GSCs were treated with 1/3 IC_{50} and 1/2 IC_{50} concentrations of GSK2126458 or LY2874455 for 24 hours. The indicated protein expression was assessed by Western blot analysis. E. GSC272 and GSC7-2 cells were implanted in the brains of immunocompromised mice (5×10^5 cells/mouse) and treated with inhibitors 5 times/week. Kaplan-Meier curves of the estimated survival durations of the study mice. In the GSC272 group, we compared control and mTOR inhibitors (*$P < 0.05$).

GSK2126458 (**Figure 4D**). Phosphorylation of FGFR1 and STAT3 was decreased in a dose-dependent fashion upon treatment with FGFR inhibitor, but phosphorylation of ERK was increased. We tested GSK2126458 and LY-2874455 *in vivo* (**Figure 4E**). GSK2126458 prolonged the survival of GSC272 but not GSC7-2 cells; LY2874455 did not prolong the survival of either of these cell lines.

Depletion of CLK2 enhanced the effect of FGFR inhibitors in GSCs

GSC272 and GSC7-2 cells with CLK2 shRNA#1 and CLK2shRNA#2 were implanted into the brains of nude mice. Each shRNA#2 GSCs led to significantly prolonged mouse survival compared to control cells (**Figure 5A**). As shown in **Figure 4E**, FGFR inhibitors had no effect on survival in GSC272 and GSC7-2 mouse models despite their *in vitro* activity as single agents.

We used PI3K/mTOR or FGFR inhibitors in CLK2-depleted cells and control cell-implanted mice. Knockdown of CLK2 led to prolonged survival but had no synergistic effect with PI3K/mTOR or FGFR inhibitors (**Figure 5B**). Combination therapy resulted in similar survival outcomes in CKL2 wildtype cells to those found in CLK2 knockdown cell lines. Although there was no significant change in CLK2 inhibition with combination therapy, tumor growth was significantly decreased after CLK2 knockdown in GSC272 mice treated with PI3K/mTOR or FGFR inhibitors compared with that in control mice (**Figure 5C**). In GSC7-2 mice, tumor growth was significantly decreased after CLK2 knockdown and PI3K/mTOR inhibitor treatment compared with vector treated controls. FGFR inhibitor treatment resulted in a significant decrease in tumor growth in CLK2 knockdown GSC272 cells compared with that in vehicle-treated cells.

Combination of CLK2 depletion with PI3K/mTOR and FGFR inhibitors blocked HIF-1alpha expression and increased the number of apoptotic cells in vivo

Individual treatment with mTOR and FGFR inhibitors had no effect on apoptosis in *in vivo,* but treatment with these agents in CLK2 knockdown tumors resulted in significant apoptotic cell death (**Figure 6A**). CLK2 knockdown prolonged animal survival, and an examination of tumors demonstrated a high level of HIF-1alpha expression. mTOR and FGFR inhibitors led to decreased HIF-1alpha expression, and the combination of CLK2 knockdown and either inhibitor decreased it further (**Figure 6B**). We confirmed HIF-1alpha expression by analyzing RPPA data *in vitro*; a heatmap demonstrated that CLK2 knockdown combined with PI3K/mTOR and FGFR inhibitors led to decreased HIF-1alpha expression (**Figure 6C**). These results showed that combination therapy had a greater effect on apoptosis and hypoxia-related resistance in the GSC mouse model.

Discussion

In our previous study, we determined CLK2's function in glioblastoma and correlated its positive expression with poor outcome [7]. CLK2 plays a role in controlling the cell cycle and survival through FOXO3a/p27. In this study, we investigated the molecular mechanism of CLK2 in GSC proliferation and identified 14-3-3τ as a significant regulator. Our results suggest that 14-3-3 proteins contribute to FOXO3 accumulation following phosphorylation by AKT.

PP2A is effective at FOXO3 dephosphorylation [22]. The results of our current study suggest that the depletion of CLK2 elevated PP2A activity, which in turn, abolished AKT phosphorylation in GSCs. Furthermore, we showed that CLK2 bound with 14-3-3α/β, 14-3-3τ, and PP-

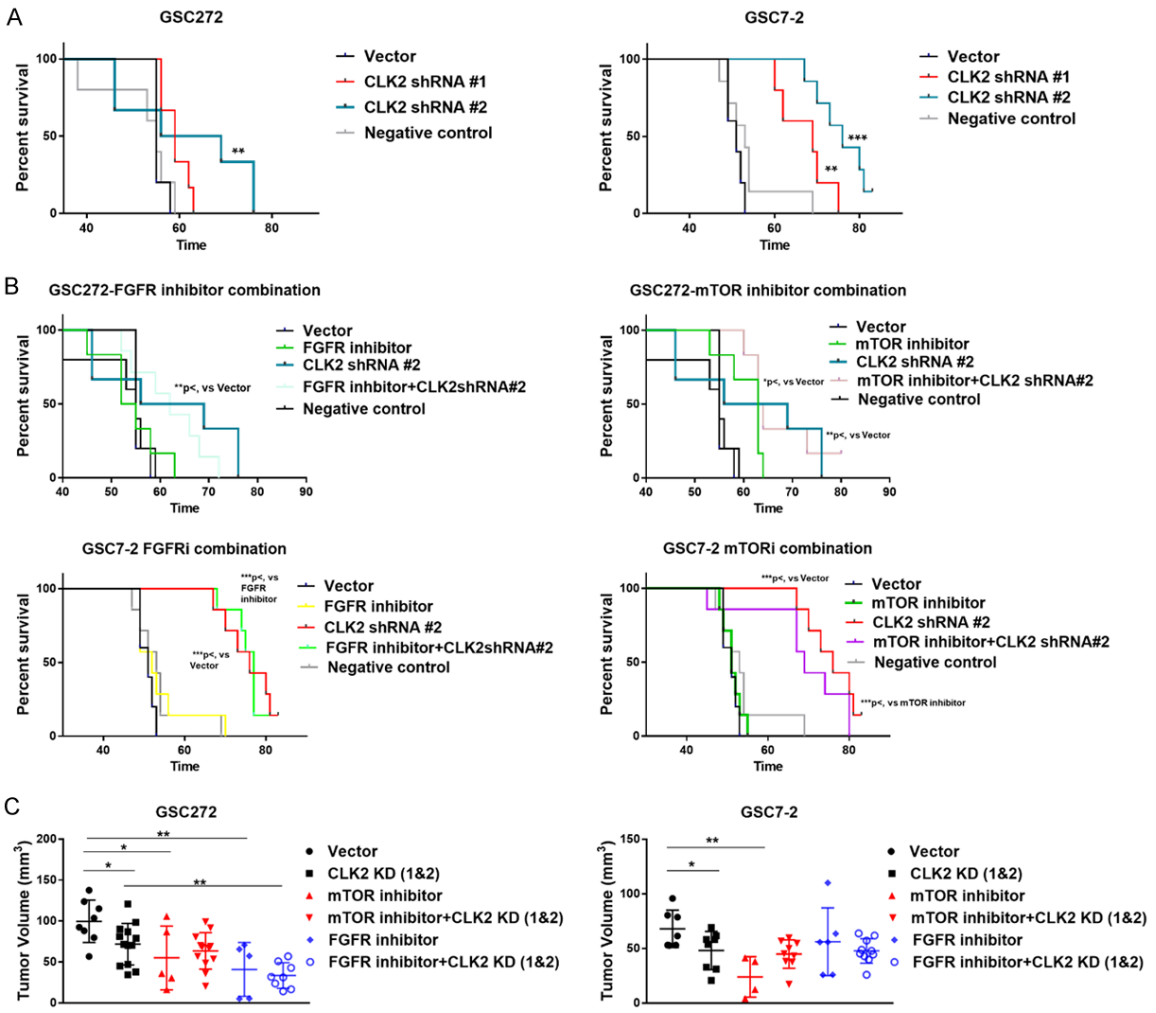

Figure 5. Effect of PI3K/mTOR or FGFR inhibitors on depletion of CLK2 GSCs and survival of mice. A, B. CLK2 knockdown or vector GSCs were implanted in the brains of immunocompromised mice; the mice were then given inhibitors 5 times/week. Kaplan-Meier curves of the estimated survival durations of study mice. In the GSC272 group, the following were compared: vector and CLK2 shRNA-infected cell implantation (**P < 0.01) and vector and PI3K/mTOR inhibitor (*P < 0.05). In the GSC7-2 mice, the following were compared: vector versus CLK2 shRNA-infected cell implantation (***P < 0.001), FGFR inhibitor versus FGFR inhibitor and CLK2 knockdown (***P < 0.001), and PI3K/mTOR inhibitor versus PI3K/mTOR inhibitor and CLK2 knockdown (***P < 0.001). C. Mice with knockdown of CLK2 (shRNA1 and shRNA2) had smaller tumors than did control mice (*P < 0.05 in GSC272 mice; *P < 0.05 in GSC7-2 mice). Treatment with PI3K/mTOR inhibitor resulted in decreased tumor size (*P < 0.05 vs vector in GSC272 mice, **P < 0.001 vs vector in GSC7-2 mice). Treatment with FGFR inhibitor resulted in decreased tumor size (**P < 0.01 vs vector in GSC272 mice; no significant difference was found in GSC7-2 mice). The combination of FGFR inhibitors and CLK2 knockdown resulted in decreased tumor size compared with CLK2 knockdown alone (**P < 0.01).

2A; 14-3-3τ had a positive binding affinity with CLK2 expression, and PP2A had a negative binding affinity in glioma cancer cells. In hepatocytes, CLK2 is upregulated by insulin induction to homeostatically regulate AKT through B56β/PP2A-mediated dephosphorylation [8]. In addition, PP2A contributes to the regulation of 14-3-3 binding to BAD [23] and the dephosphorylation of Raf-1 and KRS1 [24]. Most of the 14-3-3 binding proteins are phosphorylated either at R(S/Ar)XpSXP (mode 1) or RX(Ar/S)XpSXP (mode 2) consensus motifs [20, 25]. Besides these consensus motifs, 14-3-3 interactions are further regulated by the phosphorylation of other residues within consensus binding motifs and serine/threonine residues [26]. In this study, we established that CLK2 binds with 14-3-3 and interestingly, that CLK2 has a

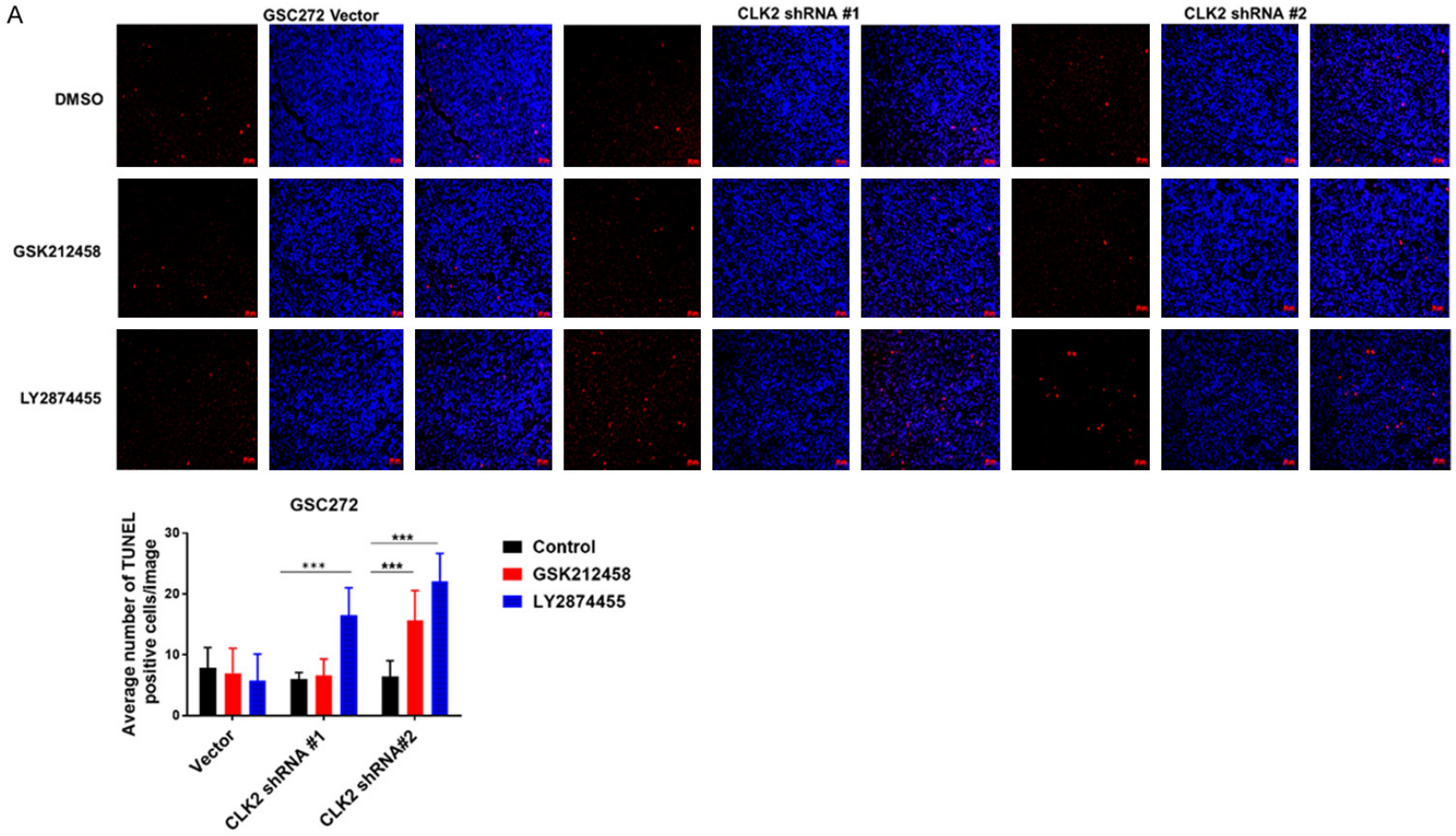
A
GSC272 Vector
CLK2 shRNA #1
CLK2 shRNA #2
DMSO
GSK212458
LY2874455
GSC272
Average number of TUNEL positive cells/image
30
20
10
0
***
***
***
Control
GSK212458
LY2874455
Vector
CLK2 shRNA #1
CLK2 shRNA#2

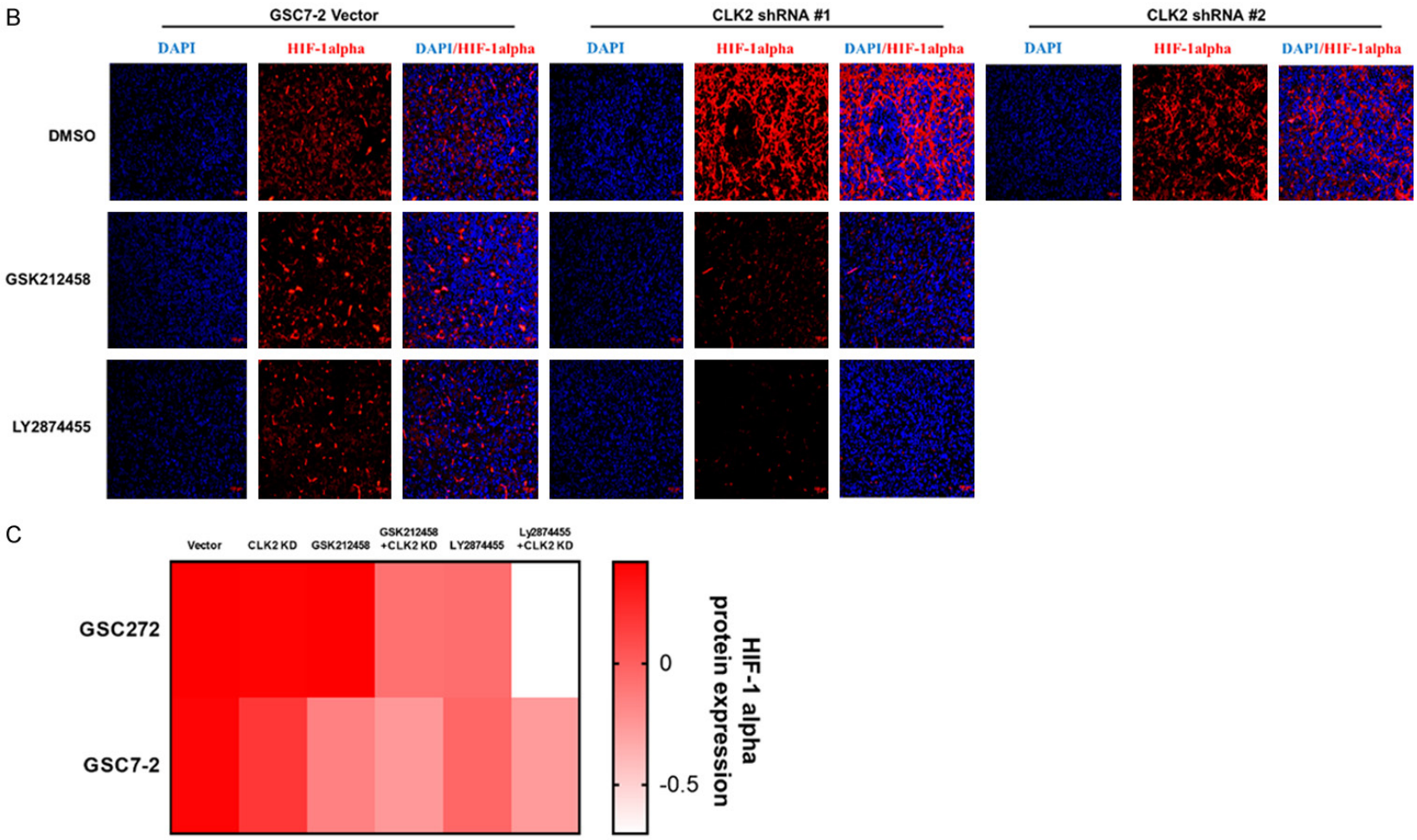

Figure 6. Treatment with inhibitor in CLK2 knockdown mice increased the number of apoptotic cells and arrested HIF-1alpha expression in vivo. A. Apoptotic cells are marked as light red dots after TUNEL staining, as observed under a fluorescent microscope. Nuclei were stained with DAPI (blue). Apoptotic cells were counted, and the number of TUNEL-positive cells was graphed. The graphs show the number of apoptotic cells ± SD (***P < 0.001). B. Immunofluorescent staining are shown for HIF-1alpha in GSC7-2 mouse glioma xenografts, with or without treatment with CLK2 knockdown or vector cells. HIF-1alpha (red) and nucleus (DAPI, blue) were expressed at CLK2 knockdown but decreased with inhibitor and combination treatment. C. The cells were treated with the IC_{50} value of inhibitors for 3 days, and the protein expression levels were analyzed by RPPA. A heatmap shows HIF-1alpha expression levels in GSC272 and GSC7-2 cells.

serine/threonine phosphorylation site. Additional studies are required to identify the phosphorylation sites that are important for CLK2's binding with 14-3-3.

The results of previous studies suggest that CLK2 protein stability is regulated by ubiquitination and proteasomal degradation [11, 21]. Indeed, co-expression of Flag-CLK2 with HA-tagged ubiquitin resulted in low levels of ubiquitination on WT CLK2. In our current study, we found high expression of CLK2; we also observed binding of CLK2 with 14-3-3 in GSCs, which prevents CLK2 ubiquitination and stabilizes CLK2 in GSCs. Interestingly, knockdown of CLK2 expression shifted binding affinity with PP2A and decreased AKT phosphorylation. 14-3-3τ (YWHAQ) is required for the G1/S transition through its role in ubiquitin-independent proteasomal degradation of p21 [27]. These results indicate that 14-3-3 protein is a master switch that leads to CLK2 stabilization and decreased PP2A activity and influences AKT phosphorylation in glioblastoma stem cells.

mTOR is downstream of the PI3K/AKT pathway, which consists of mTOR complex 1 (mTORC1) and mTOR complex 2 (mTORC2) [28]. mTORC1 activates protein translation through the phosphorylation of S6 and 4EBP1. Early-generation inhibitors of mTOR had limited antitumor activity because allosteric inhibitors such as rapamycin block mTORC1 but not mTORC2 [29]. In our study, we first confirmed the strong inhibitory effect of GSK2126458 on glioblastoma cell viability. The sensitivity of this inhibition was correlated with PTEN levels: cells with higher mRNA levels of PTEN (GSC7-2, GSC17, GSC295, and GSC28) were more resistant to GSK-2126458. DS7423 (PI3/mTOR inhibitor) was associated with PTEN alteration in glioblastoma [30]. In animal studies, 3 mg/kg of GSK-2126458 was found to result in weight loss; therefore, we decreased the dose to 1.5 mg/kg [5, 31]. More interestingly, the sensitivity of phospho-4EBP1 was correlated with the viability of GSCs. GSC20 cells were the most resistant; treatment with GSK2126458 had no effect on phosphor-4EBP1, unlike in GSC272 and GSC7-2 cells.

The mTORC1 target p-4EBP1T37/46 is a robust biomarker [32]. FGFR-TACC gene fusions in glioblastoma result in aggressive clinical behavior [33]. FGFR1 is expressed at high levels in brain tumors compared with in adjacent normal brain tissue, and its role has been established in tumorigenesis [34]. FGFR1 amplification has been found in 6% of small cell lung carcinomas [35] and is correlated with sensitivity to FGFR inhibitors [36, 37]. In our study, FGFR1 mRNA was expressed at higher levels than was the mRNA of other FGFR subtypes, and FGFR1 expression was influenced by the FGFR inhibitor LY2874455. FGFR inhibition resulted in a decrease in AKT phosphorylation, HIF-1alpha expression, and STAT3 phosphorylation. These findings suggest that FGFR inhibitor affects the STAT3/HIF-1alpha pathway *in vitro* and decreases HIF-1alpha levels *in vivo* in GSCs.

In our study, GSK2126458 and LY2874455 inhibitors had activity in GSCs *in vitro* but less significant effects in our preclinical orthotopic *in vivo* models. Since both inhibitors may have limited blood brain barrier penetration, this might account for the limited activity observed in our *in vivo* xenograft models. As with so many failed translations of studies from preclinical models to patients, future drug development should emphasize the use of agents with excellent blood-brain barrier permeability to optimize the treatment of glioblastoma.

Acknowledgements

This work was supported by the Defeat GBM Research Collaborative, a subsidiary of the National Brain Tumor Society (John de Groot), and The University of Texas MD Anderson Glioblastoma Moon Shots Program. Glioma stem cell development is funded by the MD Anderson Brain Cancer SPORE supported by P50CA127001. We thank Ningyi Tiao (Department of Neuro-Oncology, The University of Texas MD Anderson Cancer Center, Houston, TX) for sample handling and Ann Sutton (Department of Scientific Publications, The University of Texas MD Anderson Cancer Center, Houston, TX) for editorial assistance.

Disclosure of conflict of interest

None.

Address correspondence to: John F de Groot, Department of Neuro-Oncology, Unit 431, The University of Texas MD Anderson Cancer Center, 1515 Holcombe Boulevard, Houston, TX 77030, USA. Tel:

713-745-3072; Fax: 713-794-4999; E-mail: jdegroot@mdanderson.org

References

[1] Regad T. Targeting RTK signaling pathways in cancer. Cancers (Basel) 2015; 7: 1758-84.

[2] Cancer Genome Atlas Research Network. Comprehensive genomic characterization defines human glioblastoma genes and core pathways. Nature 2008; 455: 1061-68.

[3] Brennan CW, Verhaak RG, McKenna A, Campos B, Noushmehr H, Salama SR, Zheng S, Chakravarty D, Sanborn JZ, Berman SH, Beroukhim R, Bernard B, Wu CJ, Genovese G, Shmulevich I, Barnholtz-Sloan J, Zou L, Vegesna R, Shukla SA, Ciriello G, Yung WK, Zhang W, Sougnez C, Mikkelsen T, Aldape K, Bigner DD, Van Meir EG, Prados M, Sloan A, Black KL, Eschbacher J, Finocchiaro G, Friedman W, Andrews DW, Guha A, Iacocca M, O'Neill BP, Foltz G, Myers J, Weisenberger DJ, Penny R, Kucherlapati R, Perou CM, Hayes DN, Gibbs R, Marra M, Mills GB, Lander E, Spellman P, Wilson R, Sander C, Weinstein J, Meyerson M, Gabriel S, Laird PW, Haussler D, Getz G, Chin L and Network TR. The somatic genomic landscape of glioblastoma. Cell 2013; 155: 462-77.

[4] Kharas MG, Janes MR, Scarfone VM, Lilly MB, Knight ZA, Shokat KM and Fruman DA. Ablation of PI3K blocks BCR-ABL leukemogenesis in mice, and a dual PI3K/mTOR inhibitor prevents expansion of human BCR-ABL+ leukemia cells. J Clin Invest 2008; 118: 3038-50.

[5] Knight SD, Adams ND, Burgess JL, Chaudhari AM, Darcy MG, Donatelli CA, Luengo JI, Newlander KA, Parrish CA, Ridgers LH, Sarpong MA, Schmidt SJ, Van Aller GS, Carson JD, Diamond MA, Elkins PA, Gardiner CM, Garver E, Gilbert SA, Gontarek RR, Jackson JR, Kershner KL, Luo L, Raha K, Sherk CS, Sung CM, Sutton D, Tummino PJ, Wegrzyn RJ, Auger KR and Dhanak D. Discovery of GSK2126458, a highly potent inhibitor of PI3K and the mammalian target of rapamycin. ACS Med Chem Lett 2010; 1: 39-43.

[6] See WL, Tan IL, Mukherjee J, Nicolaides T and Pieper RO. Sensitivity of glioblastomas to clinically available MEK inhibitors is defined by neurofibromin 1 deficiency. Cancer Res 2012; 72: 3350-59.

[7] Park SY, Piao Y, Thomas C, Fuller GN and de Groot JF. Cdc2-like kinase 2 is a key regulator of the cell cycle via FOXO3a/p27 in glioblastoma. Oncotarget 2016; 7: 26793-805.

[8] Rodgers JT, Vogel RO and Puigserver P. Clk2 and B56beta mediate insulin-regulated assembly of the PP2A phosphatase holoenzyme complex on Akt. Mol Cell 2011; 41: 471-79.

[9] Shi Y. Serine/threonine phosphatases: mechanism through structure. Cell 2009; 139: 468-84.

[10] Kuo YC, Huang KY, Yang CH, Yang YS, Lee WY and Chiang CW. Regulation of phosphorylation of Thr-308 of Akt, cell proliferation, and survival by the B55alpha regulatory subunit targeting of the protein phosphatase 2A holoenzyme to Akt. J Biol Chem 2008; 283: 1882-92.

[11] Bidinosti M, Botta P, Kruttner S, Proenca CC, Stoehr N, Bernhard M, Fruh I, Mueller M, Bonenfant D, Voshol H, Carbone W, Neal SJ, McTighe SM, Roma G, Dolmetsch RE, Porter JA, Caroni P, Bouwmeester T, Luthi A and Galimberti I. CLK2 inhibition ameliorates autistic features associated with SHANK3 deficiency. Science 2016; 351: 1199-203.

[12] Morrison DK. The 14-3-3 proteins: integrators of diverse signaling cues that impact cell fate and cancer development. Trends Cell Biol 2009; 19: 16-23.

[13] Iwai K, Yaguchi M, Nishimura K, Yamamoto Y, Tamura T, Nakata D, Dairiki R, Kawakita Y, Mizojiri R, Ito Y, Asano M, Maezaki H, Nakayama Y, Kaishima M, Hayashi K, Teratani M, Miyakawa S, Iwatani M, Miyamoto M, Klein MG, Lane W, Snell G, Tjhen R, He X, Pulukuri S and Nomura T. Anti-tumor efficacy of a novel CLK inhibitor via targeting RNA splicing and MYC-dependent vulnerability. EMBO Mol Med 2018; 10: e8289.

[14] Tzivion G, Gupta VS, Kaplun L and Balan V. 14-3-3 proteins as potential oncogenes. Semin Cancer Biol 2006; 16: 203-13.

[15] Aitken A, Howell S, Jones D, Madrazo J and Patel Y. 14-3-3 alpha and delta are the phosphorylated forms of raf-activating 14-3-3 beta and zeta. In vivo stoichiometric phosphorylation in brain at a Ser-Pro-Glu-Lys MOTIF. J Biol Chem 1995; 270: 5706-09.

[16] Tzivion G and Avruch J. 14-3-3 proteins: active cofactors in cellular regulation by serine/threonine phosphorylation. J Biol Chem 2002; 277: 3061-64.

[17] Tzivion G, Dobson M and Ramakrishnan G. FoxO transcription factors; regulation by AKT and 14-3-3 proteins. Biochim Biophys Acta 2011; 1813: 1938-45.

[18] Brunet A, Bonni A, Zigmond MJ, Lin MZ, Juo P, Hu LS, Anderson MJ, Arden KC, Blenis J and Greenberg ME. Akt promotes cell survival by phosphorylating and inhibiting a forkhead transcription factor. Cell 1999; 96: 857-68.

[19] Lal S, Lacroix M, Tofilon P, Fuller GN, Sawaya R and Lang FF. An implantable guide-screw system for brain tumor studies in small animals. J Neurosurg 2000; 92: 326-33.

[20] Yaffe MB. How do 14-3-3 proteins work?- Gatekeeper phosphorylation and the molecular anvil hypothesis. FEBS Lett 2002; 513: 53-57.

[21] Rodgers JT, Haas W, Gygi SP and Puigserver P. Cdc2-like kinase 2 is an insulin-regulated suppressor of hepatic gluconeogenesis. Cell Metab 2010; 11: 23-34.
[22] Singh A, Ye M, Bucur O, Zhu S, Tanya Santos M, Rabinovitz I, Wei W, Gao D, Hahn WC and Khosravi-Far R. Protein phosphatase 2A reactivates FOXO3a through a dynamic interplay with 14-3-3 and AKT. Mol Biol Cell 2010; 21: 1140-52.
[23] Chiang CW, Kanies C, Kim KW, Fang WB, Parkhurst C, Xie M, Henry T and Yang E. Protein phosphatase 2A dephosphorylation of phosphoserine 112 plays the gatekeeper role for BAD-mediated apoptosis. Mol Cell Biol 2003; 23: 6350-62.
[24] Ory S, Zhou M, Conrads TP, Veenstra TD and Morrison DK. Protein phosphatase 2A positively regulates Ras signaling by dephosphorylating KSR1 and Raf-1 on critical 14-3-3 binding sites. Curr Biol 2003; 13: 1356-64.
[25] Fu H, Subramanian RR and Masters SC. 14-3-3 proteins: structure, function, and regulation. Annu Rev Pharmacol Toxicol 2000; 40: 617-47.
[26] Yaffe MB, Rittinger K, Volinia S, Caron PR, Aitken A, Leffers H, Gamblin SJ, Smerdon SJ and Cantley LC. The structural basis for 14-3-3: phosphopeptide binding specificity. Cell 1997; 91: 961-71.
[27] Wang B, Liu K, Lin HY, Bellam N, Ling S and Lin WC. 14-3-3Tau regulates ubiquitin-independent proteasomal degradation of p21, a novel mechanism of p21 downregulation in breast cancer. Mol Cell Biol 2010; 30: 1508-27.
[28] Loewith R, Jacinto E, Wullschleger S, Lorberg A, Crespo JL, Bonenfant D, Oppliger W, Jenoe P and Hall MN. Two TOR complexes, only one of which is rapamycin sensitive, have distinct roles in cell growth control. Mol Cell 2002; 10: 457-68.
[29] Sarbassov DD, Ali SM, Sengupta S, Sheen JH, Hsu PP, Bagley AF, Markhard AL and Sabatini DM. Prolonged rapamycin treatment inhibits mTORC2 assembly and Akt/PKB. Mol Cell 2006; 22: 159-68.
[30] Koul D, Wang S, Wu S, Saito N, Zheng S, Gao F, Kaul I, Setoguchi M, Nakayama K, Koyama K, Shiose Y, Sulman EP, Hirota Y and Yung WKA. Preclinical therapeutic efficacy of a novel blood-brain barrier-penetrant dual PI3K/mTOR inhibitor with preferential response in PI3K/PTEN mutant glioma. Oncotarget 2017; 8: 21741-53.
[31] Park H, Kim Y, Sul JW, Jeong IG, Yi HJ, Ahn JB, Kang JS, Yun J, Hwang JJ and Kim CS. Synergistic anticancer efficacy of MEK inhibition and dual PI3K/mTOR inhibition in castration-resistant prostate cancer. Prostate 2015; 75: 1747-59.
[32] Fan Q, Aksoy O, Wong RA, Ilkhanizadeh S, Novotny CJ, Gustafson WC, Truong AY, Cayanan G, Simonds EF, Haas-Kogan D, Phillips JJ, Nicolaides T, Okaniwa M, Shokat KM and Weiss WA. A kinase inhibitor targeted to mTORC1 drives regression in glioblastoma. Cancer Cell 2017; 31: 424-35.
[33] Di Stefano AL, Fucci A, Frattini V, Labussiere M, Mokhtari K, Zoppoli P, Marie Y, Bruno A, Boisselier B, Giry M, Savatovsky J, Touat M, Belaid H, Kamoun A, Idbaih A, Houillier C, Luo FR, Soria JC, Tabernero J, Eoli M, Paterra R, Yip S, Petrecca K, Chan JA, Finocchiaro G, Lasorella A, Sanson M and Iavarone A. Detection, characterization, and inhibition of FGFR-TACC Fusions in IDH wild-type glioma. Clin Cancer Res 2015; 21: 3307-17.
[34] Morrison RS, Yamaguchi F, Bruner JM, Tang M, McKeehan W and Berger MS. Fibroblast growth factor receptor gene expression and immunoreactivity are elevated in human glioblastoma multiforme. Cancer Res 1994; 54: 2794-99.
[35] Peifer M, Fernandez-Cuesta L, Sos ML, George J, Seidel D, Kasper LH, Plenker D, Leenders F, Sun R, Zander T, Menon R, Koker M, Dahmen I, Muller C, Di Cerbo V, Schildhaus HU, Altmuller J, Baessmann I, Becker C, de Wilde B, Vandesompele J, Bohm D, Ansen S, Gabler F, Wilkening I, Heynck S, Heuckmann JM, Lu X, Carter SL, Cibulskis K, Banerji S, Getz G, Park KS, Rauh D, Grutter C, Fischer M, Pasqualucci L, Wright G, Wainer Z, Russell P, Petersen I, Chen Y, Stoelben E, Ludwig C, Schnabel P, Hoffmann H, Muley T, Brockmann M, Engel-Riedel W, Muscarella LA, Fazio VM, Groen H, Timens W, Sietsma H, Thunnissen E, Smit E, Heideman DA, Snijders PJ, Cappuzzo F, Ligorio C, Damiani S, Field J, Solberg S, Brustugun OT, Lund-Iversen M, Sanger J, Clement JH, Soltermann A, Moch H, Weder W, Solomon B, Soria JC, Validire P, Besse B, Brambilla E, Brambilla C, Lantuejoul S, Lorimier P, Schneider PM, Hallek M, Pao W, Meyerson M, Sage J, Shendure J, Schneider R, Buttner R, Wolf J, Nurnberg P, Perner S, Heukamp LC, Brindle PK, Haas S and Thomas RK. Integrative genome analyses identify key somatic driver mutations of small-cell lung cancer. Nat Genet 2012; 44: 1104-10.
[36] Weiss J, Sos ML, Seidel D, Peifer M, Zander T, Heuckmann JM, Ullrich RT, Menon R, Maier S, Soltermann A, Moch H, Wagener P, Fischer F, Heynck S, Koker M, Schottle J, Leenders F, Gabler F, Dabow I, Querings S, Heukamp LC, Balke-Want H, Ansen S, Rauh D, Baessmann I, Altmuller J, Wainer Z, Conron M, Wright G, Russell P, Solomon B, Brambilla E, Brambilla C, Lorimier P, Sollberg S, Brustugun OT, Engel-

Riedel W, Ludwig C, Petersen I, Sanger J, Clement J, Groen H, Timens W, Sietsma H, Thunnissen E, Smit E, Heideman D, Cappuzzo F, Ligorio C, Damiani S, Hallek M, Beroukhim R, Pao W, Klebl B, Baumann M, Buettner R, Ernestus K, Stoelben E, Wolf J, Nurnberg P, Perner S and Thomas RK. Frequent and focal FGFR1 amplification associates with therapeutically tractable FGFR1 dependency in squamous cell lung cancer. Sci Transl Med 2010; 2: 62ra93.

[37] Pardo OE, Latigo J, Jeffery RE, Nye E, Poulsom R, Spencer-Dene B, Lemoine NR, Stamp GW, Aboagye EO and Seckl MJ. The fibroblast growth factor receptor inhibitor PD173074 blocks small cell lung cancer growth in vitro and in vivo. Cancer Res 2009; 69: 8645-51.